Fabrication of PdNPs Doped TiO$_2$ Nanotubes by Electroless Deposition as Hydrogen Sensor

Haidar Hameed Hamdan, Ghuson Hameed Mohammed

Abstract— **Titania nanotubes thin films have been prepared by electrochemical anodization of Ti foil at room temperature (~25ºC), in ethylene glycol base electrolyte with 0.5wt.% NH4F and 4wt% deionized water at 30V at time 3hr and then PdNPs-doped TiO2 nanotube arrays at different deposition ratio were carried out by electroless deposition. These tubes are well aligned and organized into high-density uniform arrays. The average tube diameter, ranging in size from 61 to 74 nm, the length of the tube 2.13 μ, and ranging in size of wall thickness from 21 to 29 nm. A possible growth mechanism is presented. The TiO2 nanotubes were characterized by X-ray diffraction (XRD), scanning electron microscope (FESEM) and energy dispersive X-ray spectroscopy (EDX.(The gas sensing was studied at the operating temperatures ranging from 25-350°C in different concentration hydrogen atmospheres ranging from (15, 30, 45, 60, 75ppm) H2. It was found that the TiO2 doped with Pd sensing film showed higher response of H2, with faster response time (within second) than pure TiO$_2$ sensing film. The response increased and the response time decreased with increasing of H2 concentration.**

Index Terms— **Tio$_2$ Nanotubes, Anodization, Ethylene Glycol, Electroless, Gas Sensor.**

I. INTRODUCTION

There is an ever-increasing demand for gas sensors in various fields [1,2]. Particular attention has been devoted to the monitoring of hydrogen (H2) mainly due to the wide application of hydrogen gas in either a clean energy source or in many chemical plants. As reported in many literatures, metal oxide nanofilms are potential candidates for hydrogen sensors as they played an important role in the last few years as sensing materials for various kinds of gases [3–5]. TiO$_2$-based gas sensors have been widely used because of their inert surface properties and the fact their electrical resistance could change after adsorption of hydrogen gas. For example, highly-ordered TiO$_2$ nanotubes work as a hydrogen sensor. Hydrogen molecules could be chemisorbed into the grain boundaries and pick up electrons from the conduction band to create a space charge layer among the grains. This will lead to the formation of Schottky barriers at the grain surfaces and thus a decrease of conductivity of the oxide materials [6–8]. However, as a wide band gap n-type semiconductor material, anatase TiO$_2$ (Eg ≈ 3.2eV) suffers from poor conductivity and this usually causes increased resistance of electronic components when working. Therefore, it is probably hard for anatase TiO$_2$ to be considered an ideal semiconducting material for wide use in detecting hydrogen gas. However, it has been demonstrated that element dopants can effectively address this problem. According to previous reports, TiO2 doped with metal or non-metal elements usually has a smaller grain size and a larger specific area, which leads to enhanced sensing properties in comparison with undoped TiO$_2$ [9–12].

The semiconductor gas sensors with metal catalysts is one of the most commonly used techniques for enhancing the sensitivity of gas sensors. The electrical response of a gas sensor to the target gas depends strongly on the efficiency of catalytic reactions of the surface of gas sensor material with the target gas. The sensitivity of gas sensors can be enhanced considerably by modifying the catalytic activity of the gas sensor material using metal catalysts such as Pd, Pt, Au and Ag [13,14].

In this study, we synthesize highly-ordered TiO$_2$ nanotubes by anodic oxidation of titanium foil in an aqueous solution containing 0.5wt% NH4F at ~25°C, and investigate their hydrogen sensing properties in terms of the temperature and the hydrogen concentration. The hydrogen sensing mechanism of the TiO2 nanotubes will be explained in detail.

II. EXPERIMENTAL

A. Preparation of Titania Nanotubes TiO$_2$

Pure titanium foil (99.7% purity, 0.25mm in thickness) purchased from Sigma Aldrich and cut into the desired size (20×20 mm). A direct current power supply (Agilent E3612A) was used as the voltage source for the anodization. The anodization process was carried out in a homemade plexi glass cell with two electrode configuration; titanium foil as the working electrode and 0.1 mm thick. Platinum mesh (20×30 mm) as the counter electrode under constant potential at room temperature (~25ºC). The titanium sheets were sonicated in acetone and ethanol each for (15) minutes, followed by rinsing with de-ionized (DI) water to remove the impurities and then drying in (N$_2$) gas. The anodization set-up is shown in Fig (1). The anodization was carried out at 30 Vdc, the cell electrolyte was (0.5wt%) of NH4F in ethylene glycol (95.5wt%) with (4wt%) DI water at (3hours). The prepared samples were rinsed immediately with (DI) water for several minutes and dried with high pressure (N$_2$) gas.

Haidar hameed, physics department, Baghdad University/ College of Science/ The Ministry of Higher Education and Scientific Research, Baghdad, The Republic of Iraq.
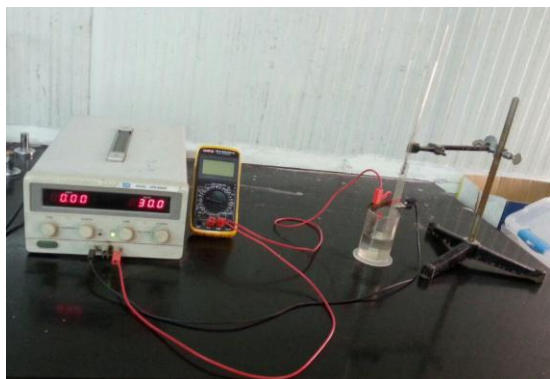
Ghuson Hameed, physics department, Baghdad University/ College of Science/ The Ministry of Higher Education and Scientific Research, Baghdad, The Republic of Iraq.

Fabrication of PdNPs Doped TiO₂ Nanotubes by Electroless Deposition as Hydrogen Sensor

Fig 1: Apparatus Set-Up of Titanium Anodization Experiment.

B. Preparation of PdNPs/TiO₂ Catalysts

After anodizing of titanium, the samples were ultrasonically cleaned in distilled water for 10-20 min to remove surface debris. Then the TiO₂ nanotubes sample were immerged into the bath for electroless deposition.

The titania nanotubes samples were immerged into two separate solutions, solutions (A and B). One was the palladium ion solution (solution A), which was prepared by dissolving the palladium chloride (0.2g) in Ethylenediaminetetraacetic acid disodium salt dehydrate (4 g), the distilled water (90 ml) and aqueous ammonia (10ml) were used to adjust the pH to the range of 10-10.6. The solution was sonicated for 20 min until palladium chloride is fully dissolved (orange color). Sample of titania nanotubes were then soaked in the PdC_{l2} solution. After several mints, the titania samples was also washed with immersion in distilled water.

While the other was a reducing agent solution (solution B). The reducing agent that we used for this work was hydrazine (10ml) with distilled water (90ml) and aqueous ammonia (10ml), the chemical reaction started within 1min, and the sample turned to dark silver instantaneously, then obtained PdNPs/TiO₂ sample was washed also washed with immersion in water. All this process carried out at a constant temperature of 60 °C.

In order to reach rates fixed by weight of doping noble metal (palladium) on the layer of titania nanotubes i.e. values that we adopt in this paper, namely, (0.3, 0.5, 0.7, 0.9 and 1.1 wt. %), we did more experience and solutions to the way deposition electroless metal (palladium) and examined by (EDX) to determine the proportion of metal doping, and we got the conditions that lead to get these percentages of doping metals.

C. Physical Characterization

For the structural and morphological characterization of the anodized samples, top views were recorded by scanning electron microscopy (FESEM) using JEOL JSM-6510LVF FEG-SEM, (USA), and (AFM) study carried out by (AA3000, Angstrom Advanced Inc. USA). The crystallographic structures of the samples were determined using Ultima IV X-ray diffractometer of 1.5406 Å from Cu-k α (supplied by Rigaku Co.), USA.
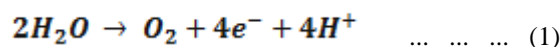
Then the hydrogen sensing measurements were carried out using aluminum as electrodes in the temperature range of 25-150°C. The sensing element was placed in a flow type homemade chamber. A Keithley 6517A Electrometer/High Resistance Meter was used to test the resistance variation of the nanotube sensor in alternating atmospheres of air and dilute H2 (15, 30, 45, 60, 75ppm). During the measurements, the temperature of the sensor was controlled with a Lakeshore 340 temperature controller.
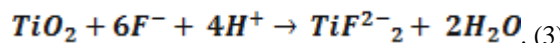
III. RESULTS AND DISCUSSIONS

A. Synthesis of Titania Nanotubes:

Titania nanotubes were fabricated at different conditions in glycerol-based electrolytes and the effect of water content was investigated. In general in the absence of water in electrolytes and presence it, the anodization process will suffer from lack of H+ ions and also high viscosity of the solution which leads to the formation of titanium dioxide layers only. The overall reaction for anodic oxidation of titanium can be represented as [15]:

$$2H_2O \rightarrow O_2 + 4e^- + 4H^+ \qquad \dots \dots \dots (1)$$

$$Ti + O_2 \rightarrow TiO_2 \qquad \dots \dots \dots \dots \dots (2)$$

In the initial stages of the anodization process, field-assisted dissolution dominates chemical dissolution due to the relatively large electric field across the thin oxide layer (the resistance to the current is minimum). Small pits formed due to the localized dissolution of the oxide, represented by the following reaction, act as pore forming centers[15]:

$$TiO_2 + 6F^- + 4H^+ \rightarrow TiF^{2-}_2 + 2H_2O \quad (3)$$

The pits convert to bigger pores and the pore density increases. Subsequently, the pores spread uniformly over the surface, as show in SEM and AFM resulted.

The current transients recorded during anodization of Ti at 30V for 3 hours in electrolytes consisting of ethylene glycol, 0.5wt.% NH4F, are shown in Fig (2).
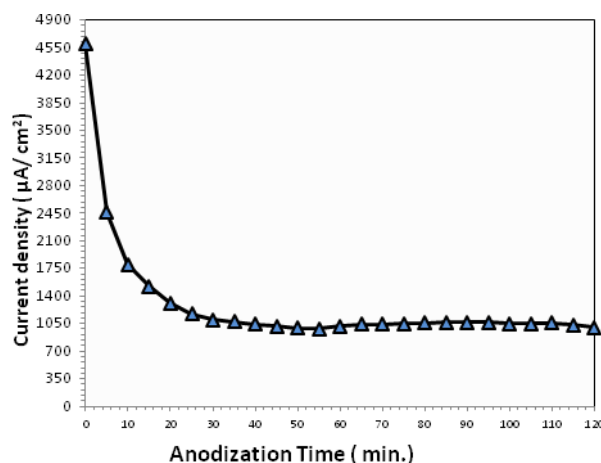

Fig 2: The current transients recorded during 3 hours of Ti anodization at 30V.

The current-time characteristics during the Titania formation where recorded as shown in next sections. In general the current density starts at a high magnitude then it reduces gradually with time then became nearly constant (steady state), this agrees with the explanation in a previous work [16],

Field emission scanning electron microscopy (FESEM) images of a typical TiO₂ nanotubes array is shown in Fig (3a).

The optimized anodization conditions applied have resulted in the formation of TiO_2 nanotubes (hollow cylinders) perpendicular to the substrate, were open at the top and closed at the bottom. These TiO_2 nanotubes are well-aligned and organized into a highly oriented array. From image a dark region is visible in the middle of each nanotube probably reflecting the hollow tubular structure.

FESEM examinations revealed that the nanotubes, with an average diameter of $\approx$ 74 nm and a height of $\approx$ 3.2 μm, Figs (3 b-f) shows FESEM images with different magnifications of typical TiO_2 nanotube layers covered with Pd nanoparticles at different doping ratios (0.3, 0.5, 0.7, 0.9 and 1.1 wt.%), respectively. The electroless-deposited Pd formed nanoparticles, the nucleation of the Pd takes place randomly on the surface of the nanotubes which diameter varies from 19 to 27 nm, which changes with the doping ratios, some Pd nanoparticles were gathered on the pore openings and showed a distribution more dense with increasing doping ratios, while some were deposited into the nanotubes. Also we observed of the palladium nanoparticles are located at the top edges of the nanotubes, on their side walls and on the exterior mouth of the TiO_2 nanotubes. TiO_2 nanotubes covered with Pd nanoparticles with increasing of doping ratios exhibit quite a different morphology. The Pd particles are agglomerated and in the form of rings at the top of the nanotubes. The amount of Pd is here so high, that it results in a visible reduction of their internal diameter of titania nanotubes, as shown Table (1), this agrees with the explanation in a previous work [17,18],

Table 1: The average diameter, inner diameter, wall thickness and grain size of un-doped TiO_2 nanotubes and PdNPs/TiO_2 nanotubes at different doping ratios

sample	Diameter (nm)	Inner diameter (nm)	Wall thickness (nm)	G. Size of Pd (nm)
Un-doped TiO_2	74	63	11	= =
PdNPs/TiO_2 at 0.3 wt.%	76	54	22	19
PdNPs/TiO_2 at 0.5 wt.%	77	48	29	20
PdNPs/TiO_2 at 0.7 wt.%	82	44	38	22
PdNPs/TiO_2 at 0.9 wt.%	83	38	45	25
PdNPs/TiO_2 at 1.1 wt.%	84	35	49	27

Fig (4 a-f) shows the two-dimensional (2D) and three-dimensional (3D) AFM images of the un-doped and Pd nanoparticles-doped TiO2 nanotubes layer by electroless deposition at ratios (0.3, 0.5, 0.7, 0.9 and 1.1 wt.%), respectively.

The 2D images show that the films are uniform and the titania layer surface is well covered with grains that are almost uniformly distributed over the surface. The 3D images

exhibit large nicely separated conical columnar grains in all thin films. The average surface roughness and the average grain size increases from 2.3 nm to 14.45 nm and from about 64.51 nm to 91.22 nm with increase of the Pd nanoparticles content, as shown in Table (2). This may be due to the bigger clusters formed by the coalescence of two or more grains, this result is in agreement with the previous work [19,20].

Table 2: Morphological characteristics from AFM images for TiO_2 nanotubes and doped PdNPs/TiO_2 nanotubes**.**

Sample	Grain size of Pd (nm)	Roughness average (nm)	Root mean square (RMS) (nm)
Un-doped TiO_2	= =	2.3	3.03
PdNPs/TiO_2 at 0.3 wt.%	64.51	5.31	7.43
PdNPs/TiO_2 at 0.5 wt.%	66.68	7.67	9.79
PdNPs/TiO_2 at 0.7 wt.%	72.92	10.63	12.62
PdNPs/TiO_2 at 0.9 wt.%	76.25	12.11	14.51
PdNPs/TiO_2 at 1.1 wt.%	91.22	14.45	19.55

In general, as the doping ratios of Pd nanoparticles increases on titania layer, the RMS and roughness of the PdNPs/TiO_2 nanotubes and the grain size increase.

EDX (energy dispersive X-ray microanalysis) was recorded in the binding energy region of 0 - 14keV. The result is shown in Fig (5) and Table (3). The peak from the spectrum reveals the presence of four peaks around 4.56, 0.433, 0.421 and 0.325 keV, respectively. The intense peaks are assigned to the Ti and the less intense one to the surface TiO_2. The peaks of Pd are distinct at 2.8, 2.7 and 0.26 keV. This result confirms the existence of Pd atoms in the TiO_2 nanotubes, this agrees with the explanation in a previous work [21,22].

Table 3: Energy dispersive X-ray spectroscopy results of un-doped TiO_2 nanotubes and PdNPs/TiO_2 doped at different doping ratios

.

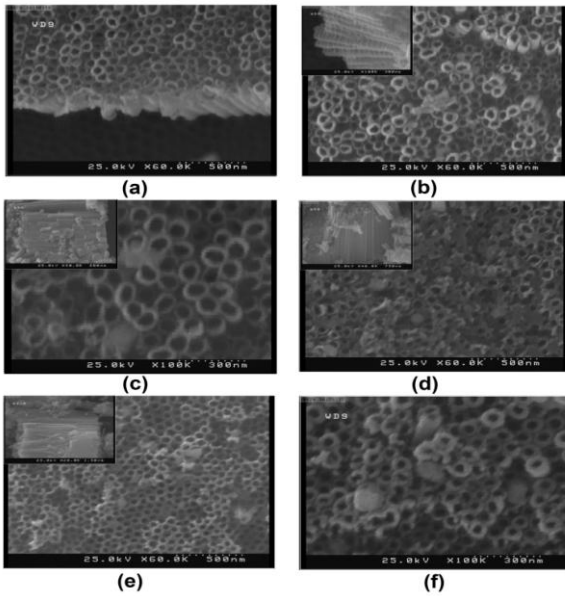| Sample	Titanium (Ti) w%	Oxygen (O) w%	Dopant (Ag) wt%
Un-doped TiO_2	74.4	25.6	0
PdNPs/TiO_2 at 0.3 wt.%	74.6	25.1	0.3
PdNPs/TiO_2 at 0.5 wt.%	74.1	25.4	0.5
PdNPs/TiO_2 at 0.7 wt.%	73.1	26.2	0.7
PdNPs/TiO_2 at 0.9 wt.%	74.5	24.6	0.9
PdNPs/TiO_2 at 1.1 wt.%	73.3	25.6	0.11

Fig 3: FESEM images of (a) un-doped TiO$_2$ nanotubes (top view), (b) PdNPs/TiO$_2$ nanotubes (top view) and (Insert of cross section) at 0.3 wt.%, (c) PdNPs/TiO$_2$ nanotubes (top view) and (Insert of cross section) at 0.5 wt.%, (d) PdNPs/TiO$_2$ nanotubes (top view) and (Insert of cross section) at 0.7 wt.%, (e) PdNPs/TiO$_2$ nanotubes (top view) and (Insert of cross section) at 0.9 wt.%, (f) PdNPs/TiO$_2$ nanotubes (top view) at 1.1 wt.%.
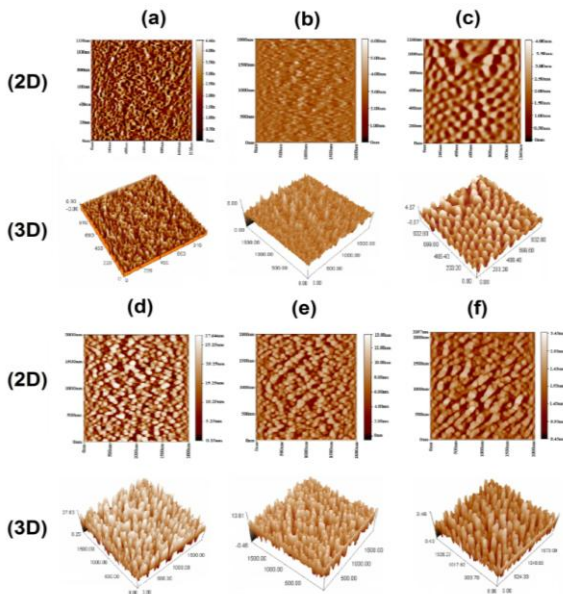

Fig 4: 2D and 3D AFM images of (a) TiO$_2$ nanotubes, (b) PdNPs/TiO$_2$ nanotubes at 0.3 wt.%, (c) PdNPs/TiO$_2$ nanotubes at 0.5 wt.%, (d) PdNPs/TiO$_2$ nanotubes at 0.7 wt.%, (e) PdNPs/TiO$_2$ nanotubes at 0.9 wt.%, (f) PdNPs/TiO$_2$ nanotubes at 1.1 wt.%.
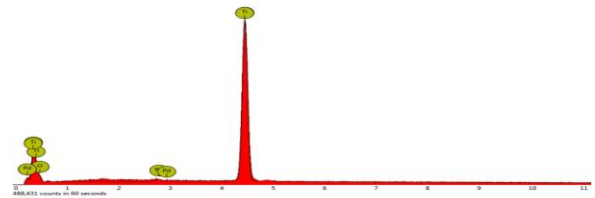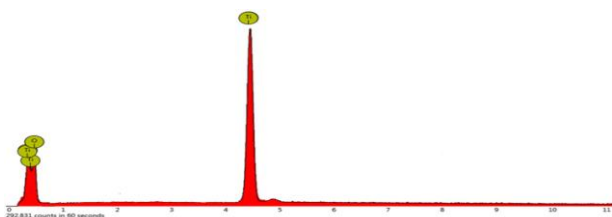

Fig 5: EDX analysis of (a) un-doped TiO$_2$ nanotubes, (b) PdNPs/TiO$_2$ nanotubes at 0.9 wt.%.

Throughout studying the X-ray diffraction spectrum, we can understand the crystalline growth nature of TiO$_2$ nanotubes prepared by anodization method and Pd nanoparticles deposition on TiO2 nanotubes layers by electroless method at different doping ratios (0.3, 0.5, 0.7, 0.9 and 1.1 wt.%).

The XRD analysis of the TiO$_2$ nanotubes and PdNPs/TiO$_2$ nanotubes. Fig (6) shows the X-ray diffraction patterns of the un-doped and palladium doped TiO$_2$ at different doping ratios. From the wide angle XRD pattern, the titania samples exist only in anatase phase, with their characteristic diffraction peaks of 2θ values.

In consequence, the prepared TiO$_2$ nanotubes (pattern a) and PdNPs/TiO$_2$ nanotubes (pattern b-f) at different doping ratios are well-crystallized pure anatase form. In comparison with XRD pattern of un-doped TiO$_2$, Pd loaded on TiO$_2$ surface nearly has no influence on crystalline structure. Pd phase has not been detected in the XRD patterns of PdNPs/TiO$_2$ nanotubes, possibly because the Pd content on TiO2 surface is not enough to form clearly crystalline, but this can be seen when increasing the doping ratio leads to increased (FWHM) of anatase peaks.

Or accurate interpretation, the XRD patterns didn't show any Pd phase (even for the 1.1 wt.% Pd-doped TiO$_2$). This may reveal that Pd ions are uniformly dispersed in TiO$_2$ matrix. In the region of 2θ° = 10° - 80°, the shape of diffraction peaks of the crystal planes of un-doped TiO2 is quite similar to those of Pd/TiO$_2$ of different doping ratios. The average crystal size of TiO$_2$ and Pd doped TiO$_2$ nanoparticles were calculated and also, were presented in Table (4). The average crystal size was not significantly changed due to the addition of the Pd+2, this agrees with the exploitation in a previous work[23-24].
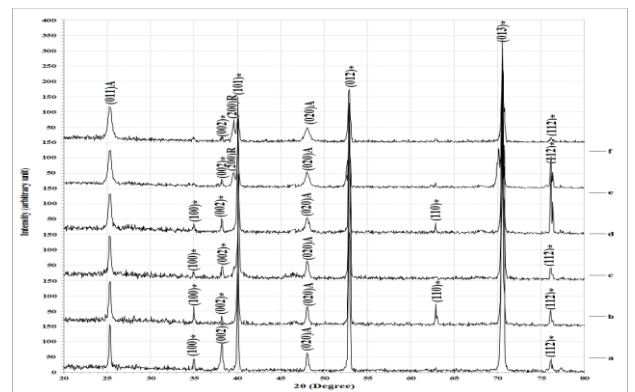

Fig 6: XRD patterns of (a) un-doped TiO$_2$ nanotubes, (b) PdNPs/TiO$_2$ nanotubes at 0.3 wt.%, (c) PdNPs/TiO$_2$ nanotubes at

0.5 wt.%, (d) PdNPs/TiO$_2$ nanotubes at 0.7 wt.%, (e) PdNPs/TiO$_2$ nanotubes at 0.9 wt.%, (f) PdNPs/TiO$_2$ nanotubes at 1.1 wt.%.

B. Hydrogen sensing properties

Fabricated PdNPs-doped TiO$_2$ nanotubes were converted into the gas sensor device. Finally, these devices were placed to gas sensor testing cell.

Fig (7) shows typical response curves of the titania nanotubes sensor tested with the reducing atmosphere containing (75ppm) hydrogen in air. It was found that the titania nanotube sensor presented a good response working at temperatures (50-300°C). The resistance of sensor increased rapidly after exposure to hydrogen-containing atmosphere. The sensor presented a linear drift of the sensor's resistance. At the relatively lower working temperature of 100°C, the response time (the time required for the sensor to reach 90% of the saturation value) of the PdNPs-doped TiO$_2$ nanotube was around 100 seconds and a change in resistance was found. After the working temperature increased to 200°C, the response time was still around 80 seconds but the change in resistance increased.

The sensitivity, response and recovery characteristics of the sensor device have been studied by measuring the change in resistance, in the ambient and reducing gas atmosphere. The gas detection sensitivity (S) of the sensor device has been evaluated using the relation[26]:

$$S = (R_a - R_g)/R_g \qquad \ldots \ldots \ldots \ldots (4)$$

where Ra and Rg are resistance values of the sensor device in the ambient and reducing gas atmosphere, respectively.

Gas sensing tests were conducted by measuring the change in resistance under gas exposure in a temperature range from room temperature to 300°C, where the maximum sensitivity about 59% was obtained at 250°C, as shown in Fig (2). Sensitivity at temperatures higher than 250°C were not reported because the change in resistance was very small at higher temperatures. We found the conductivity of sensor increased at 250°C, thereby resistance decreased by a factor of three, whereas maximum sensitivity obtained up to the saturation at this temperature level. The optimum temperature for the sensor was 250°C, beyond which the sensor sensitivity was degrade because of the dissociation activity of H2 with PdNPs/TiO$_2$. At higher temperature the reactivity rate decreased with hydrogen adsorption and desorption and the sensor failed to reach an equilibrium state [27]. Fig (8) elucidates dynamic repeatable signal with the short response time (tres) and recovery time (trec) for sensor device under (75ppm) H2 at 250°C. There was a dramatic change in response/recovery time after 100°C, as described before by chemical bonding study [5].When the sensor was in hydrogen off-state, the open surface of PdNPs/TiO$_2$ adsorbed oxygen adsorbates, such as O2-, O- and O2. Surface chemisorbed oxygen vacancies depend ubiquitously on grain size and closed pack facets which drastically varies with temperature. At low temperatures the adsorbates remain in a weak physisorbed bonding state with sensor surface. The more the temperatures the more strength gets the bonding between chemisorbed ions and the surface [27]. However, each grain size on the surface has its own capability for adsorbing oxygen ions and the sensor reaches its maximum

saturation level by balancing the H$_2$ adsorption reactivity with temperature; thus, sensor response/recovery time may fluctuate due to incomplete desorption of gas [28]. Subsequently at 300°C the device response was smaller than at 250°C and reached 16% after long response/recovery times. The dynamic response of the PdNPs/TiO$_2$ based sensor is given in Fig (9) with (15, 30, 45, 60, 75ppm) gas concentration.
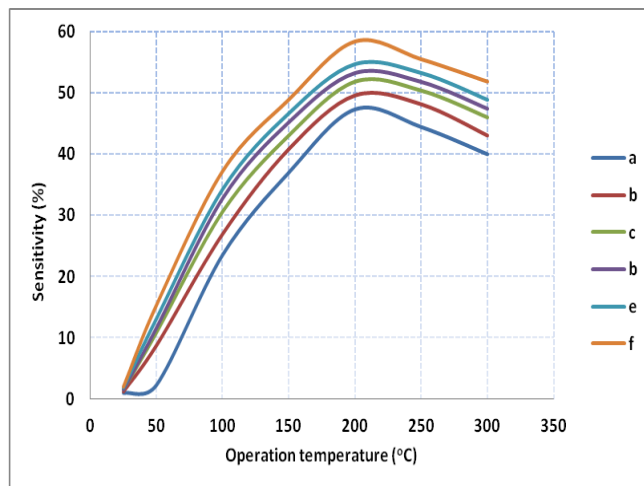

Fig 7: Sensitivity with different working temperatures of the(a) un-doped TiO$_2$ nanotubes, (b) PdNPs/TiO$_2$ nanotubes at 0.3 wt.%, (c) PdNPs/TiO$_2$ nanotubes at 0.5 wt.%, (d) PdNPs/TiO$_2$ nanotubes at 0.7 wt.%, (e) PdNPs/TiO$_2$ nanotubes at 0.9 wt.%, (f) PdNPs/TiO$_2$ nanotubes at 1.1 wt.%.
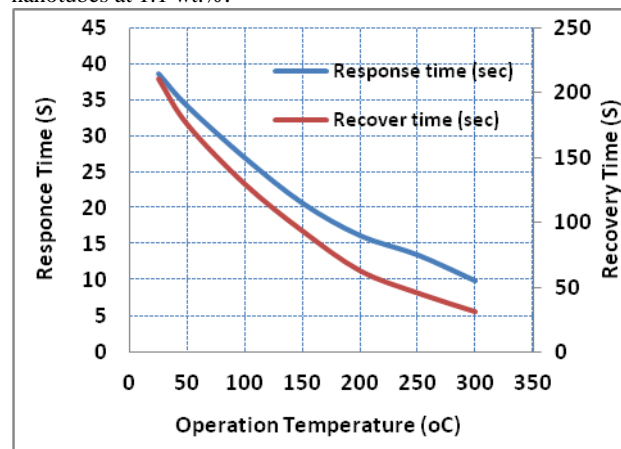

Fig 8: Response time of the PdNPs/TiO$_2$ with concentration (0.9 wt.%) at different working temperatures.
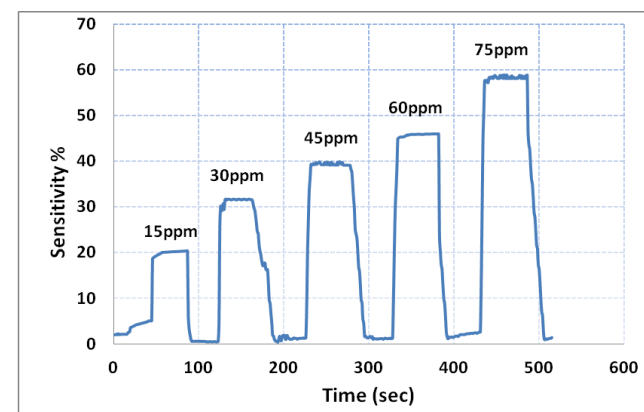
Fig 9: Sensitivity behavior of PdNPs/TiO$_2$ thin film at (0.9 wt.%) to thin film to different hydrogen concentrations. The bias voltage was 6 v with the temperature set to 200°C.

IV. CONCLOSIONS

Semiconductor gas sensors based on nano-crystalline TiO2 nanotube thin films are fabricated with the anodization method. palladium doped of titania nanotubes by electroless deposition process. The deposition of PdNPs via electroless method here was found to be an effective method to titania nanotubes for gas sensor. Round-shaped and uniformly distributed nanoparticles were deposited on the surface of the pore walls of titania nanotubes. Tunability of the concentration of nanoparticles on the titania surface can be achieved by changing the deposition time of PdCl2 or time of immersion of titania sample in the deposition solution. The EDX and FESEM analysis showed the presence of metallic Pd in the pores, and no chlorine was detected.

The PdNPs for hydrogen sensing applications lies in the fact that the hydrogen dissociation occurs on Pd while the reactions resulting in resistance changes take place on the metal oxides. In other words, the specially separated step-wise reactions need a highly efficient path way to deliver the dissociated hydrogen atoms generated by the first step for the next step reaction. the novelty of this sensor reflects in the fact that a high and fast response can be obtained even when the working temperature is as low as 50-75C. The greatly enhanced hydrogen sensing performance of the directly formed composite indicates that the direct formation of shape-controlled Pd nanocrystals on metal oxides may be an effective and workable strategy to fabricate high-performance low-temperature hydrogen sensors. The sensor response was measured and analyzed for H2 concentrations at (15, 30, 45, 60, 75ppm) in the temperature range $(25 - 300°C)$.

The sensor fabricated from these PdNPs/TiO2 exhibited high sensitivity and rapid response/recovery to hydrogen at 250 °C. The highest sensitivity was about 81% when the sensor was exposed to 75 ppm, and the response and recovery times were about 20 and 30 s, respectively. The PdNPs/TiO2 sensors showed fast response times toward hydrogen even at low operating temperatures. These results demonstrate that Pd doped TiO2 nanotubes can be used as the sensing material for fabricating high performance hydrogen sensors. Besides, hydrogen gas sensing mechanism of the sensor was studied and a model proposed.

REFERENCES

[1] Zakrzewska, K. Mixed oxides as gas sensors. Thin Solid Films 2001, 16, 229–238.

[2] Williams, D.E. Semiconducting oxides as gas-sensitive resistors. Sens. Actuators B 1999, 57, 1–16.

[3] Zheng, Q.; Zhou, B.; Bai, J.; Li, L.; Jin, Z.; Zhang, J.; Li, J.; Liu, Y.; Cai, W.; Zhu, X. Self-organized TiO2 nanotube array sensor for the determination of chemical oxygen demand. Adv. Mater. 2008, 20, 1044–1049.

[4] Sun, Y.-F.; Liu, S.-B.; Meng, F.-L.; Liu, J.-Y.; Jin, Z.; Kong, L.-T.; Liu, J.-H. Metal oxide nanostructures and their gas sensing properties: A review. Sensors 2012, 12, 2610–2631.

[5] Shimizu, Y.; Kuwano, N.; Hyodo, T.; Egashira, M. High H2 sensing performance of anodically oxidized TiO2 film contacted with Pd. Sens. Actuators B 2002, 83, 195–201.

[6] Hazra, S.K.; Basu, S. High sensitivity and fast response hydrogen sensors based on electrochemically etched porous titania thin films. Sens. Actuators B 2006, 115, 403–411.

[7] Li, Z.; Ding, D.; Ning, C. P-Type hydrogen sensing with Al- and V-doped TiO2 nanostructures. Nanoscale Res. Lett. 2013, 81, doi:10.1186/1556-276X-8-25.

[8] Şennik, E.; Çolak, Z.; Kılınç, N.; Öztürk, Z.Z. Synthesis of highly-ordered TiO2 nanotubes for a hydrogen sensor. Int. J. Hydrogen Energy 2010, 35, 4420–4427.

[9] Atashbar, M.Z.; Sun, H.T.; Gong, B.; Wlodarski, W.; Lamb, R. XPS study of Nb-doped oxygen sensing TiO2 thin films prepared by sol-gel method. Thin Solid Films 1998, 326, 238–244.

[10] Ok, K.C.; Park, J.; Lee, J.H.; Ahn, B.D.; Lee, J.H. Semiconducting behavior of niobium-doped titanium oxide in the amorphous state. Appl. Phys. Lett. 2012, 100, 142103.

[11] Boon-Bretta, L.; Bousek, J.; Moretto, P. Reliability of commercially available hydrogen sensors for detection of hydrogen at critical concentrations: Part II—Selected sensor test results. Int. J. Hydrogen. Energy 2009, 34, 562–571.

[12] Hübert, T.; Boon-Brett, L.; Black, G.; Banach, U. Hydrogen sensors—A review. Sens. Actuators B 2011, 157, 329–352.

[13] Sunghoon Park; Soohyun Kim; Suyoung Park; Wan In Lee; Chongmu Lee, " Effects of Functionalization of TiO2 Nanotube Array Sensors with Pd Nanoparticles on Their Selectivity ", Sensors; Sep2014, Vol. 14 Issue 9, p15849.

[14] Haidar Hameed. Hamdan, Seyed Ali Hoseini, Marwa Abdul Muhsien, "Palladium–Doped SnO2 Nanostructure Thin Film Prepared Using SnCl4 Precursor for Gas Sensor Application", Proceedings of the 4th International Conference on Nanostructures (ICNS4) 12-14 March, 2012, Kish Island, I.R. Iran.

[15] Haidar Hameed Hamdan, "Fabrication of TiO2 Nanotubes Using Electrochemical Anodization" M.Sc. thesis, College of Science, Baghdad University, (2012).

[16] Haidar Hameed Hamdan, Hareith I. Jaafar, Abdulalkareem M. A. Alsammerraei, "Study of the effect of NH4F concentration on the structure of electrochemically prepared TiO2 nanotubes", Iraqi Journal of Science. Vol 53.No 2.2012.Pp 827-831.

[17] J. L. Fransaer and R. M. Penner // J. Phys. Chem. B 103 (1999) 7643.

[18] T. Hirsch, M. Zharnikov, A. Shaporenko, J. Stahl, D. Weiss, O. S. Wolfbeis and V. M. Mirsky // Angew. Chem. Int. Ed. 44 (2005) 6775.

[19] Y. Fu, L. Zhang and J. Zheng // J Nanosci Nanotechnol. 5 (2005) 558.

[20] D.V. Goia // J. Mater. Chem. 14 (2004) 451.

[21] Zhongliang Shi , Jerzy A. Szpunar, "Synthesis of an ultra-thin palladium membrane for hydrogen extraction ", Rev. Adv. Mater. Sci. 15(2007) 1-9.

[22] M. G. Hosseini; M. M. Momeni, " Design of Highly Uniform Platinum and Palladium Nanoparticle Decoration on TiO2 Nanotube Arrays: An Efficient Anode to the Electro-Oxidation of Alcohols ", Journal of Ultrafine Grained and Nanostructured Materials, Vol. 1, No. 1, 2012, PP. 23-27.

[23] Ahmed A. Abd El-Rady, Mahmmoud S. Abd El-Sadek, Mohamed M. El-Sayed Breky, Fawzy H. Assaf, " Characterization and Photocatalytic Efficiency of Palladium Doped-TiO2 Nanoparticles ", Advances in Nanoparticles, 2013, Vol.2, No.4, 372-377.

[24] Fereshteh Chekin, Samira Bagheri, Sharifah Bee Abd Hamid "Synthesis and spectroscopic characterization of palladium-doped titanium dioxide catalyst", Bulletin of Materials Science April 2015, Volume 38, Issue 2, pp 461-465.

[25] M. G. Hosseini, M. M. Momeni and M. Faraji, "Palladium Nanoparticle Supported on TiO2 Nanotubes as New Catalysts for Hydrazine Electro-oxidation", International Journal of Pure & Applied Chemistry Vol. 7 , No. 1, 2012 pp. 65-71.

[26] Haidar Hameed Hamdan, Marwa Abdul Muhsien , Evan T. Salem, Ibrahim R. Agool, "Gas sensing of Au/n-SnO2/p-PSi/c-Si heterojunction devices prepared by rapid thermal oxidation", Applied Nanoscience August 2014, Volume 4, Issue 6, pp 719-732.

[27] Yanrong Wang, Bin Liu, Songhua Xiao, Han Li, Lingling Wang, Daoping Cai, Dandan Wang,a Yuan Liu, Qiuhong Li and Taihong Wang, " High performance and negative temperature coefficient of low temperature hydrogen gas sensors using palladium decorated tungsten oxide" J. Mater. Chem. A, 2015,3, 1317-1324

[28] Yamauchi M, Kobayashi H, Kitagawa H." Hydrogen storage mediated by Pd and Pt nanoparticles. "ChemPhysChem 2009;10:2566–76.

Haidar Hameed Hamdan, PhD in physics, University of Baghdad, Assistant Lecturer at the Faculty of Science / Baghdad University, I have a lot of published research in the fields of (Solar cell fabrication and characterization, Semiconductors science (thin film, characterization, application, device, etc.), Gas sensors, Nanotechnology science). In addition to posts at numerous international conferences.